Journal of Electrical Engineering, Vol. 77, No. 2, 2026, pp. 130-138
https://reference-global.com/journal/JEE

Insulation diagnosis of power semiconductor using a PCB based microstrip patch-type partial discharge sensor

Gyeong-Yeol Lee[1], Sung-Wook Kim[2*]

Printed circuit board (PCB) based power semiconductors are essential elements in modern electrical systems by their fast and reliable capabilities within compact miniaturized sizes. However, due to the recent trends of increased operating voltage and frequency ranges, the dielectric strength of insulation systems in PCBs has been faced a lot of challenges regarding degradation and acceleration of insulation properties, initiating partial discharges (PD). This paper proposes a PCB based microstrip patch-type PD sensor to detect high frequency PD signals generated from insulation defects. Four typical types of PCB defect models were fabricated to simulate the insulation defects within the power semiconductor. Phase-resolved partial discharge (PRPD) patterns were obtained at 120% of each partial discharge inception voltage (PDIV) level, and various statistical PD features were extracted to establish PD datasets. Four representative machine learning (ML) algorithms were comparatively analyzed, and the random forest (RF) model achieved the highest performance with an accuracy of 96.9%.

Keywords: Power semiconductor, partial discharge, microstrip patch-type PD sensor, PCB defect, insulation diagnosis

1 Introduction

In modern electrical systems, power semiconductors have been widely employed owing to their compact size, fast switching capability, and excellent reliability [1-3]. In particular, the advent of wide-bandgap (WBG) devices, such as silicon carbide (SiC) and gallium nitride (GaN), has significantly improved the capabilities and performances of power semiconductor technologies. These WBG-based power semiconductors can operate under high voltage (HV) and high frequency switching conditions, offering remarkable advantages in efficiency, compactness, and overall functionality in the power systems [4, 5].

In recent decades, as the application ranges of power semiconductors continue to expand, insulation reliability within the power semiconductors has become a critical factor for stable operations. However, the elevated operating voltage and switching frequency levels lead to exposing a lot of electrical and mechanical stress to the insulation materials, which can induce internal defects and accelerate insulation degradation, eventually resulting in the initiation of partial discharge (PD). Although numerous studies have investigated PD measurement techniques using electrical, thermal, and acoustic methods, there still remains many challenges in practical applications due to the limited installation spaces and increasing complex and miniaturization of printed circuit board (PCB) based power semiconductors. Furthermore, it has not been established standardized procedures or diagnostic criteria for PD measurement in the power semiconductors [6-9].

A lot of studies have been conducted to diagnose insulation defects using various kinds of machine learning (ML) algorithms. In [10, 11], researchers used multilevel pulse width modulation (PWM) waveforms to simulate switching voltage conditions (dv/dt) on typical insulation defects within the power semiconductors, such as void and crack, and applied representative ML algorithms, including random forest (RF) and artificial neural network (ANN) models, to classify types of insulation defects. In [12], researchers obtained phase-resolved partial discharge (PRPD) patterns of various types of PD defects within insulation systems and were used artificial intelligence (AI) based ML algorithms for PD classification. However, from the perspective of reliable operations of the power semiconductors, PD characteristics of various types of insulation defects have to be investigated. To address these challenges, this paper presents the insulation diagnosis using a PCB based microstrip patch-type PD sensor capable of high-frequency PD signals generated from insulation defects. Four representative defect models were prepared to simulate the typical insulation defects within the power semiconductors. Distinguishable PD features were extracted from PRPD patterns for defect models. Four machine learning (ML) algorithms were applied for

[1] Korea Hydro & Nuclear Power Co., LTD (KHNP), Gyeongju 38120, Republic of Korea
[2*] Department of Electrical and Electronics Engineering, Silla University, Busan 46958, Republic of Korea
gyeongyeollee1@gmail.com, number1@silla.ac.kr

https://doi.org/10.2478/jee-2026-0014, Print (till 2015) ISSN 1335-3632, On-line ISSN 1339-309X

defect classification, and their performances were compared using statistical indices.

Chapter 2 introduces a microstrip patch-type PD sensor, proposed in this study. Chapter 3 describes the experimental setups and procedures used to simulate various types of insulation defects occurring in power semiconductors. Chapter 4 presents PRPD patterns and extracted distinguishable features corresponding to each defect model. Chapter 5 compares insulation diagnosis results of representative ML algorithms including performance evaluation using multiple statistical evaluation indices.

2 Design and fabrication of microstrip patch-type PD Sensor

Figure 1 shows the photograph and configuration of the microstrip patch-type PD sensor, used in this paper. The sensor was designed on a standard plane FR-4 substrate with a thickness of 1.0 mm and a relative permittivity (ε_r) of 4.4, which is commonly used in PCB manufacturing due to its cost effectiveness and ease of fabrication. The radiating patch and the feed elements were designed on both sides of the substrate based on bipolar microstrip feed geometric structure using a copper cladding with a thickness of 35 μm. A 50 Ω SMA connector was directly mounted between the radiating patch and feed elements to connect with the measuring equipment.

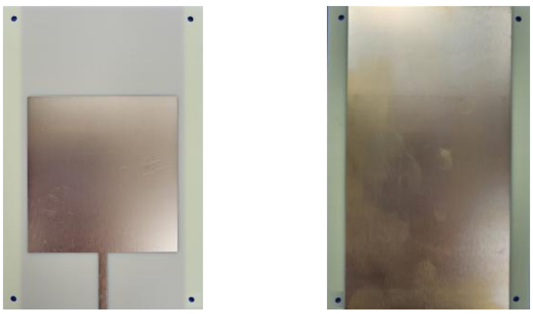

(a) Photograph

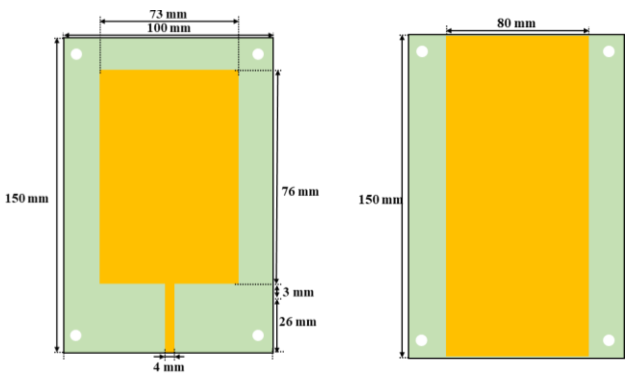

(b) Configuration

Fig. 1. Microstrip patch-type PD sensor

To evaluate the impedance matching between the microstrip patch-type PD sensor and the measurement equipment, a return loss was measured using a vector network analyzer (VNT, 37347C, Anritsu, Japan). A lower value indicates reduced reflected power and more efficient signal transfer into the sensor [13]. Figure 2 shows the return loss. The return losses in a frequency range of less than 1 GHz were lower than –20 dB while the return losses in a frequency range of higher than 1 GHz were about –10 to –20 dB.

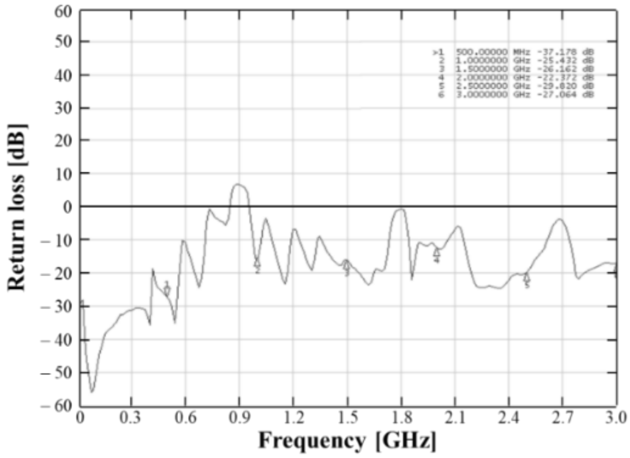

Fig. 2. Return loss

3 Experimental setup and methods

3.1 Insulation defect models

Figure 3 shows a typical configuration of multilayer PCB, composed of multiple prepreg and core layers with copper traces. It plays essential roles in structural integrity with mechanical strength and stability and electrical interconnections. Modern PCBs have evolved from single- or double-sided designs to multilayer configurations to offer high power densities and switching frequencies in compact power semiconductors [14, 15].

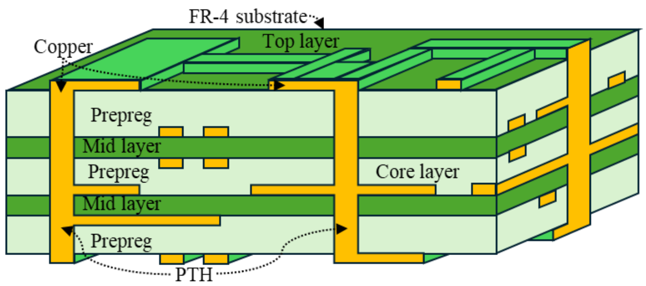

Fig. 3. A configuration of the multilayer PCB

Figure 4 presents a cross-sectional diagram of the multilayer PCB. In modern power systems, miniaturized PCB designs has become an essential requirement for achieving high integration density, reduced system volume, and improved operational efficiency. The spacing between adjacent copper traces is typically within tens to a few hundreds of micrometers. Despite significant advances in the electrical and mechanical properties of PCB insulation materials, the compact geometry intensifies local electric fields within narrow insulation gaps, which can lead to partial discharges and reduced dielectric strength, eventually compromising system reliability [16-19].

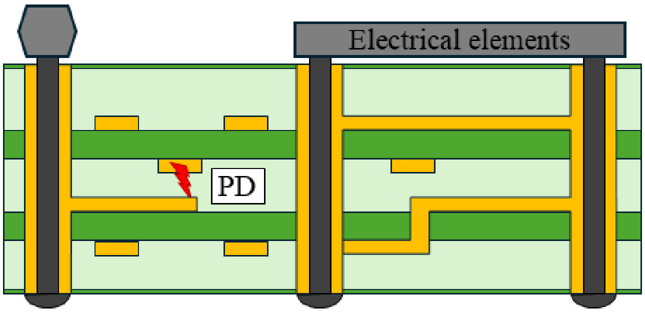

Fig. 4. A cross-sectional diagram of the PCB

To simulate the various kinds of design cases of copper traces, four different defect models were prepared. Figure 5 shows photographs and drawings of typical insulation defect cases within the PCBs [7]. A plane to plane (PP) defect was designed to simulate parallelly positioned copper wires, as shown in Fig. 5(a). Similarly, a right angle to right angle (RA) defect was designed to simulate parallelly positioned copper wires with a corner of 90 angles, as shown in Fig. 5(b). A vertex to plane (VP) and plane to vertex (PV) defects were designed to simulate incorporations of right-angled edged copper wires with plane copper wires, as shown in Fig. 5(c) and (d), respectively. Gaps between the HV and ground electrodes were uniformly set at 500 µm. All electrodes were made of 1 ounce copper cladding on fire resistance (FR-4) substrate with a thickness of 1.0 mm. To minimize the unexpected external corona and field enhancement, all edges were rounded.

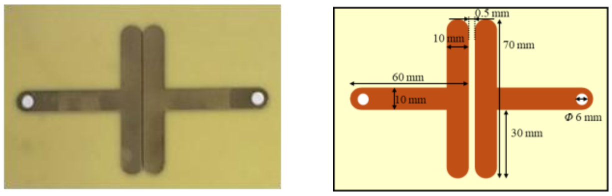

(a) Plane to plane (PP) defect

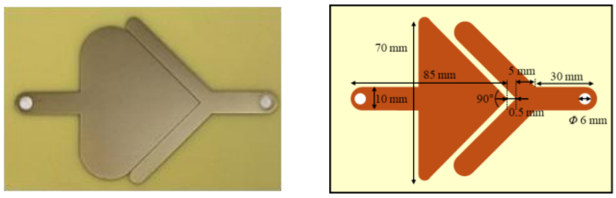

(b) Right angle to right angle (RA) defect

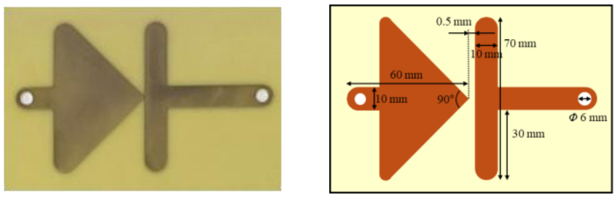

(c) Vertex to plane (VP) defect

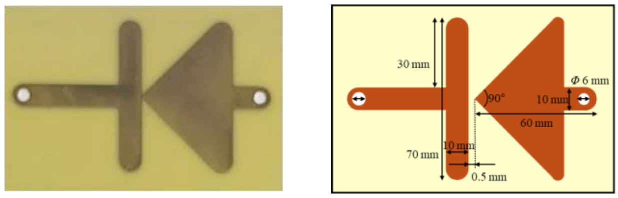

(d) Plane to vertex (PV) defect

Fig. 5. Photographs and drawings of defect models

3.2 PD simulation test setup

Figure 6 illustrates the photograph and configuration of experimental setup used in this paper. An oil-immersed HV transformer with maximum output voltage of 20 kV and output current of 100 mA (Model 720-1, Hipotronics, CT, USA) was used to apply HV source and the applied voltage levels were adjusted by the AC regulator. A microstrip patch-type PD sensor was parallelly positioned at a distance of 40 mm to measure the EM waves generated from the defect models, and the outputs were recorded using a digital storage oscilloscope (DSO, MSO 5204B, Tektronix Inc., USA) with a maximum sampling rate of 10 GS/s. The measured PD signals were compared to 1 nF coupling capacitor with a high-precision measurement device (MPD 600, Omicron Corp., Austria) as the conventional electrical detection method based on IEC 60270 standard.

The external noises were lower than 3 mV for the microstrip patch-type PD sensor and 2 pC for the MPD 600. To ensure experimental consistency and reproducibility, all conditions were kept constant for the measurement processes.

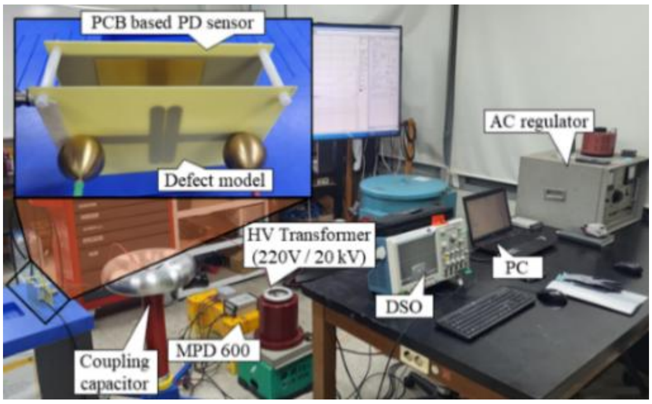

(a) Photograph

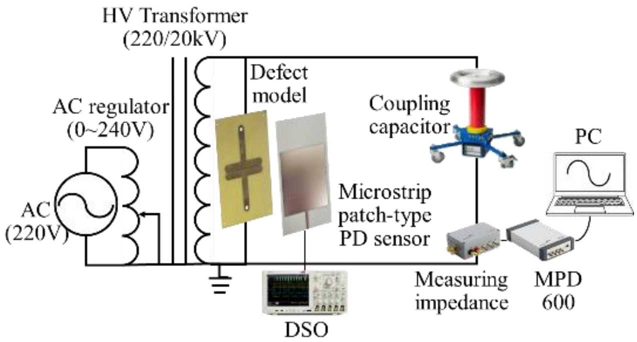

(b) Configuration

Fig. 6. Experimental setup

As mentioned above, the microstrip patch-type PD sensor measures the electromagnetic waves generated from the insulation defects. To evaluate the output characteristics of the microstrip patch-type PD sensor in accordance with the injected artificial calibration PD pulses, the output voltages were measured using a pulse generator (UPG 620, Omicron Corp., Austria) ranging from 2 to 6 V with a rising time of several nanoseconds. Fig. 7 shows example waveforms of injected artificial calibration PD pulse of 5 V and its output signal of the microstrip patch-type PD sensor. From the output signal evaluation test, it was confirmed that the microstrip patch-type PD sensor, used in this paper, had a linear response in accordance with the injected calibration PD pulses, as shown in Fig. 8.

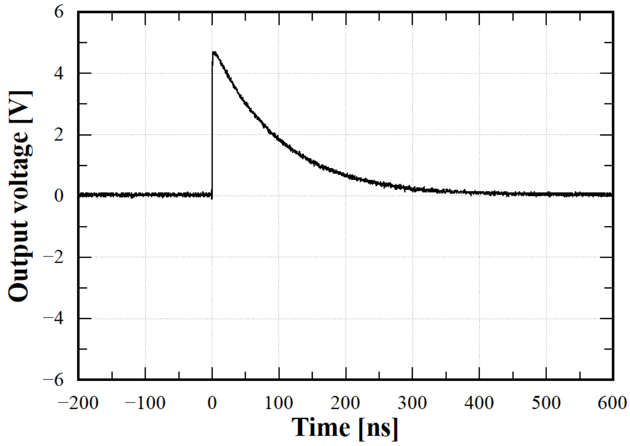

(a) Calibration pulse

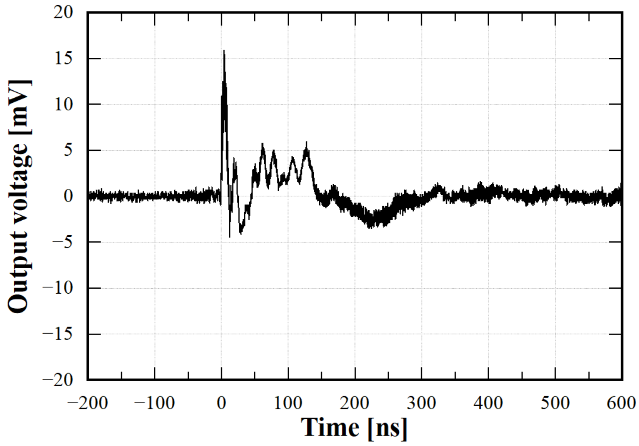

(b) Output signal

Fig. 7. Example waveforms of the calibration pulse and output signal

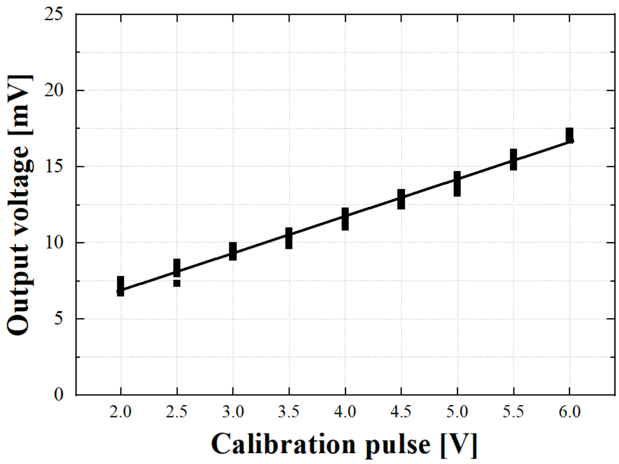

Fig. 8. Linearity of microstrip patch-type PD sensor

3.3 PD simulation test process

Figure 9 shows the PD simulation test process for defect classification within the power semiconductors. Firstly, the applied voltage was increased by 0.5 kV steps and maintained at least 1 minute for stabilization. Once the measured PD signals was higher than the environmental noise level, in this paper 3 mV, the applied voltage level was set as the PDIV and increased to 120% of the PDIV for PD signal recording. A total of 400 PRPD patterns were recorded and processed to extract distinguishable PD features. Each PRPD pattern was recorded for 60 seconds at the commercial system frequency of 60 Hz, corresponding to over 3,600 voltage cycles, ensuring sufficient statistical representation of PD activities. All extraction processes were conducted under consistent and controlled conditions. Based on the extracted features, PD dataset was established. After then, four different kinds of ML algorithms were applied to classify the types of PD defects. To compare and evaluate the performance of ML algorithms, various kinds of evaluation indices were calculated.

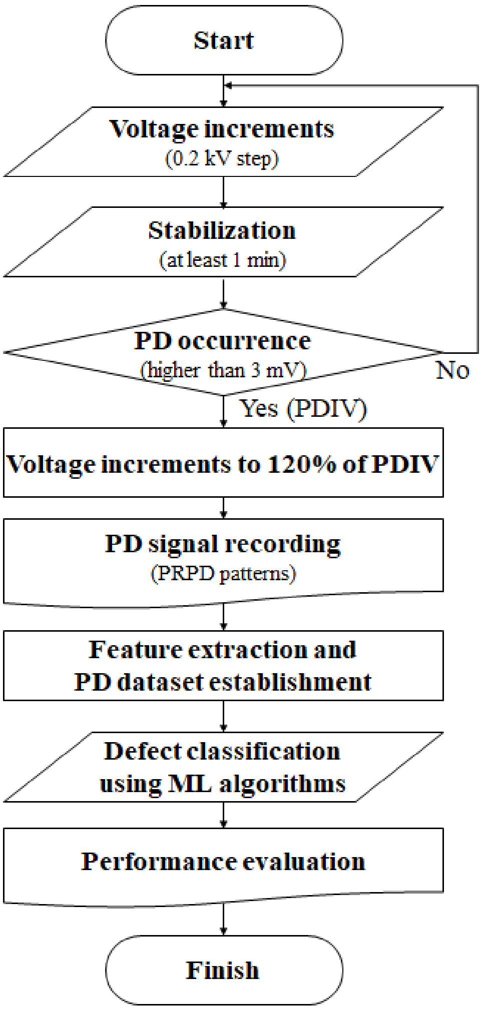

Fig. 9. Experimental setup

4 PD measurements and feature extraction

Since PD mechanisms vary depending on insulation defect types and applied voltage magnitudes, PRPD pattern analysis have been widely used as an effective diagnostic approach for identifying and classifying insulation defects based on characteristic phase and amplitude distributions of PDs [17].

Figure 10 shows the PRPD patterns measured at 120% of each PDIV for each defect model using the conventional electrical detection method (MPD 600) and the microstrip patch-type PD sensor.

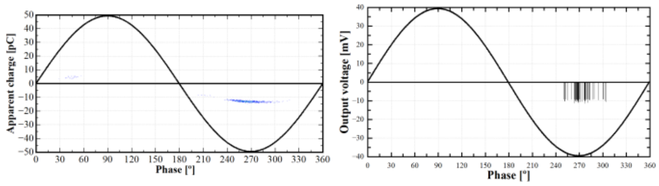

(a) PP defect

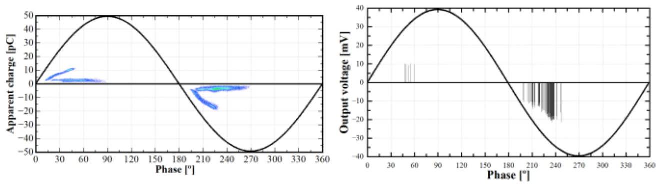

(b) RA defect

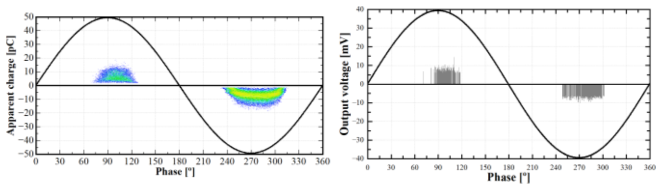

(c) VP defect

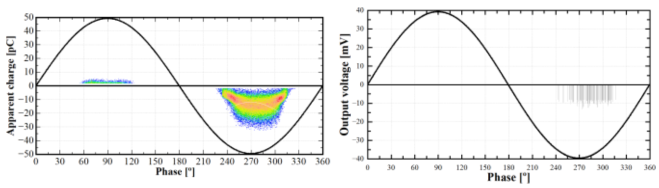

(d) PV defect

Fig. 10. PRPD patterns

The applied voltage and apparent charge levels were 3.8 kV and 16.2 pC for PP defect, 3.2 kV and 23.1 pC for RA defect, 2.8 kV and 19.4 pC for VP defect, and 3.2 kV and 32.8 pC for PV defect, and the corresponding output magnitudes of the microstrip patch-type PD sensor were 10.8 mV, 15.4 mV, 8.9 mV, and 9.2 mV, respectively. For the PP and PV defects, the PD pulses measured using MPD 600 were observed in both the negative and positive half-cycles, whereas the PD pulses, measured by the proposed PD sensor, were pre-dominantly observed in the negative half-cycle. The corresponding phase angles of the PD sensor were 244° to 317° for the PP defect and 248° to 318° for the PV defect, respectively. For RA and VP defects, the PD pulse distributions of the PD sensor were narrower than those of MPD 600. The corresponding phase angles of the PD sensor were 47° to 61° and 197° to 248° for the RA defect and 72° to 117° and 248° to 305° for the VP defect, respectively. These differences may originate from the electromagnetic detection principle of the proposed sensor, which is sensitive to high-frequency components of PD signals.

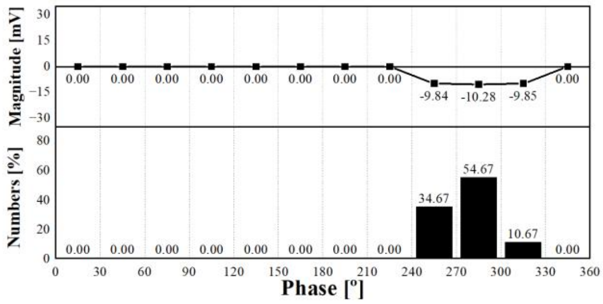

(a) PP defect

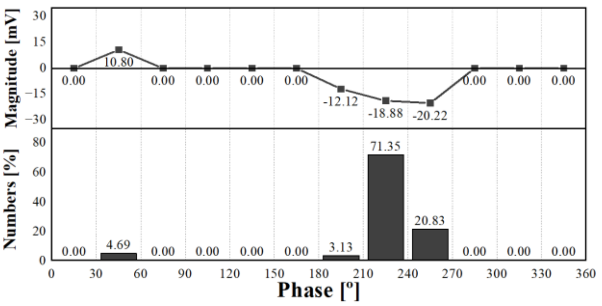

(b) RA defect

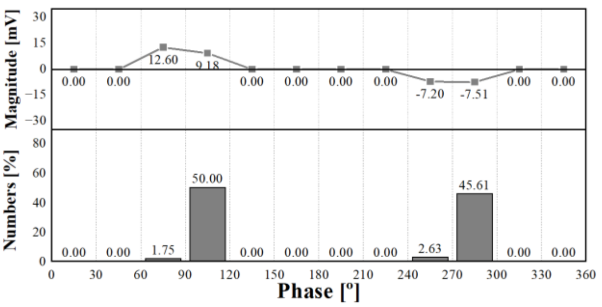

(c) VP defect

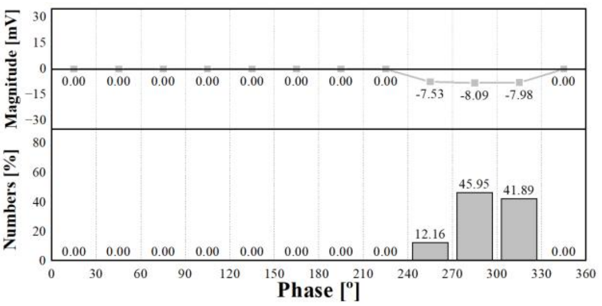

(d) PV defect

Fig. 11. PD features extracted from PRPD patterns

Figure 11 shows the average magnitudes and pulse count ratios distributed over 30° phase intervals. For the PP and PV defects, PD pulses were exclusively observed near the peak region of the applied voltage in the negative polarity. In contrast, for the RA defect, more than 95% of the PD pulses were concentrated in the rising region of the negative polarity. In contrast to the other defects, the PRPD pattern obtained from the VP defect exhibited PD activities in both positive and negative polarities, showing a relatively symmetric distribution with respect to the voltage phase.

5 Insulation diagnosis

PD feature dataset, established in the previous chapter, was divided into training sub-dataset (80%) and testing sub-dataset (20%) [18]. To ensure reliable generalization performance, a 10-fold cross-validation was employed. Then, four representative ML algorithm models, including RF, k-nearest neighbor (KNN), support vector machine (SVM), and ANN, were applied to classify typical insulation defects within PCB structures. The performance results of each model were evaluated using statistical indices such as accuracy, error rate, sensitivity, precision, specificity, and F1-score.

RF model is an ensemble-based classifier that aggregates predictions from multiple decision trees trained on bootstrap subsets, thereby reducing variance through bagging. It is inherently robust to feature scaling and effectively captures nonlinear interactions via its hierarchical tree structure, providing stable generalization even with redundant or correlated features. KNN model is a non-parametric, instance-based classifier that assigns class labels by majority voting among k nearest samples. It performs well for locally clustered data and complex decision boundaries but is sensitive to high-dimensional spaces and outliers. SVM constructs an optimal separating hyperplane that maximizes the margin between classes using linear and RBF kernels. It is highly effective in high-dimensional feature spaces with well-separated decision boundaries but depends on appropriate kernel and parameter selection. ANN is a multilayer perceptron with two to three hidden layers using ReLU activation and dropout regularization. It effectively learns nonlinear relationships but requires sufficient data to prevent overfitting and ensure convergence [17, 18, 23-25].

Figure 12 shows the accuracies and error rates of each ML algorithm. Accuracy and error rate indices were used to assess the overall performance and quantify the misclassifications of algorithms, respectively. The KNN model showed the second highest accuracy of 90.0%, while the SVM and ANN models showed the accuracy of 89.4%, the lowest accuracy among the ML algorithms.

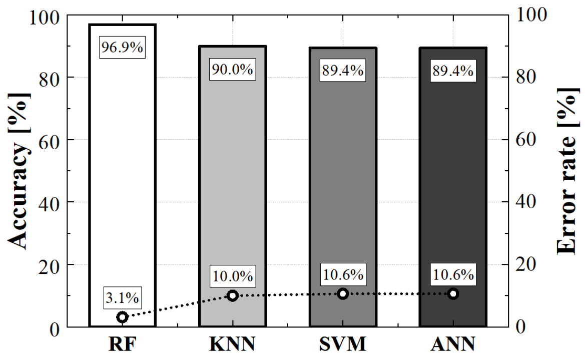

Fig. 12. Accuracies and error rates

In addition, various kinds of statistical indices, including sensitivity (recall), precision specificity, and F1-score, were employed to evaluate the overall performances in accordance with ML algorithms. Sensitivity (recall) and precision indices were applied to calculate corrected detections in actual positives and predicted positives, while specificity index was used to calculate correct actual negatives. F1-score index was employed to evaluate the balances between precision and recall [26-29]. As shown in the performance evaluation results in Fig. 13, RF model, in this paper, showed the highest accuracy of 96.9% and the highest F1-score of 0.968, demonstrating the most balanced classification among all algorithms.

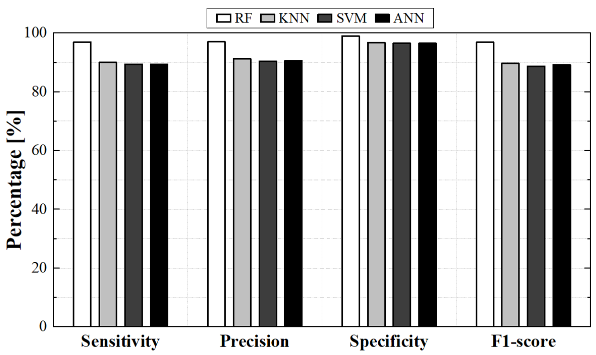

Fig. 13. Performance evaluation results

6 Discussion and conclusions

This paper deals with insulation diagnosis within PCB-based power semiconductors using a PCB-based microstrip patch-type PD sensor. Four representative defect models were designed to simulate typical electric field concentrations occurring between copper traces in multilayer PCB structures.

Based on the PD simulation tests, it was confirmed that the PRPD patterns exhibited distinct phase-resolved characteristics and discharge activities depending on the defect type. The PP and PV defects showed PD activities predominantly in the negative half-cycle, whereas the RA and VP defects generated PD pulses in both positive and negative half-cycles. Various PD features were systematically extracted from the PRPD patterns and constructed the comprehensive PD feature dataset. Subsequently, four ML algorithm models were comparatively evaluated for insulation defect diagnosis. Among them, the RF model achieved the highest classification accuracy and F1-score, demonstrating superior robustness as well as a balanced performance in terms of sensitivity and specificity. The superiority was attributed to the ensemble-based decision-making mechanism of the RF model, which improves the generation by reducing the variance based on the aggregation of multiple decision trees. As a result, the RF model was concluded to be the most robust and practically viable classifier for the given PD datasets.

From the experimental results, the microstrip patch-type PD sensor demonstrated effective detection capability for PD signals generated from insulation defects within PCB structures, indicating its strong potential for application in compact and highly integrated PCB-based power semiconductor designs. Since the experiments were conducted under controlled conditions, which may not fully reflect the electrical, thermal, and electromagnetic environments encountered in actual power semiconductor modules, further investigations are required to conduct under realistic operating conditions, including high switching frequencies, elevated temperatures, and compact sized packaging structures. In addition, future work will be conducted focusing on optimizing sensor geometry for higher bandwidth response and integrating sensing and classification algorithms into embedded systems for extension of the diagnostic framework. In addition, considering practical operational conditions of the PCB-based power semiconductor modules, PD characteristics under fast switching PWM voltages with high dv/dt and elevated temperatures will be investigated.

References

[1] G.-M. Ma, H.-Y. Zhou, C. Shi, Y.-B. Li, Q. Zhang, C.-R. Li, "Distributed Partial Discharge Detection in a Power Transformer Based on Phase-Shifted FBG," *IEEE Sensors Journal*, vol. 18, no. 7, pp. 2788-2795, Apr. 2018.

[2] H. Wen, X. Li, F. Zhang, Z. Qu, Y. Jiang, N. Luo, G. Wang, X. Wang, W. Liu, M. Cui, Y. Zhao, "Junction Temperature Extraction for Silicon Carbide Power Devices: A Comprehensive Review," *IEEE Transactions on Power Electronics*, vol. 40, no. 2, pp. 3090-3111, Feb. 2025.

[3] D. Cooper, "Power Module Integration: A new approach," *IEEE Power Electronics* Magazine, vol. 3, no. 3, pp. 31-36, Sep. 2016.

[4] R. Singh, P. Paniyil, Z. Zhang, "Transformative Role of Power Electronics: In solving climate emergency," *IEEE Power Electronics Magazine*, vol. 9, no. 2, pp. 39-47, June 2022.

[5] A.B. Jørgensen, S. Bęzkowski, C. Uhrenfeldt, N.H. Petersen, S. Jørgensen, S. Munk-Nielsen "A Fast-Switching Integrated Full-Bridge Power Module Based on GaN eHEMT Devices," *IEEE Transactions on Power Electronics*, vol. 34, no. 3, pp. 2494-2504, Mar. 2019.

[6] N. Wang, I. Cotton, J. Robertson, S. Follmann, K. Evans, D. Newcombe, "Partial Discharge Control in a Power Electronic Module Using High Permittivity Non-linear Dielectrics," *IEEE Transactions on Dielectrics and Electrical Insulation*, vol. 17, no. 4, pp. 1319-1326, Aug. 2010.

[7] T.-C. Tai, S.-Y.A. Bao, B.K. Boyanapalli, C.-C. Kuo, C.-K. Chang, "Partial Discharge Inception and Breakdown Voltage Analysis in PCB-Based Electrode Structures," *Applied Sciences*, vol. 15, no. 4, pp. 2115, Feb. 2025.

[8] N.M. Vichare, M.G. Pecht, "Prognostics and Health Management of Electronics," *IEEE Transactions on Components and Packaging Technologies*, vol. 29, no. 1, pp. 222-229, Mar. 2006.

[9] C. Li, Y. Yang, G. Xu, Y. Zhou, M. Jia, S. Zhong, Y. Gao, C. Park, Q. Liu, Y. Wang, S. Akram, X. Zeng, Y. Li, F. Liang, B. Cui, J. Fang, L. Tang, Y. Zeng, X. Hu, J. Gao, G. Mazzanti, J. He, J. Wang, D. Fabiani, G. Teyssedre, Y. Cao, F. Wang, Y. Zi, "Insulating materials for realising carbon neutrality: Opportunities, remaining issues and challenges," *High Voltage*, vol. 7, no. 4, pp. 610-632, Aug. 2022.

[10] E. Balouji, T. Mckelvey, "Classification of Partial Discharges Originating From Multilevel PWM Using Machine Learning," *IEEE Transactions on Dielectrics and Electrical Insulation*, vol. 29, no. 1, pp. 287-294, Feb. 2002.

[11] E. Balouji, T. Hammarström, T. McKelvey, "Partial Discharge Classification in Power Electronics Applications using Machine Learning," *2019 IEEE Global Conference on Signal and Information Processing (GlobalSIP)*, Ottawa, ON, Canada, 11-14 Nov. 2019.

[12] M.R.K. Shagor, F. Haque, "A Partial Discharge Classification Approach in Shipboard Power System Under Power Electronics Switching Voltage," *2025 IEEE Electric Ship Technologies Symposium (ESTS)*, Alexandria, VA, USA, 5-8 Aug. 2025.

[13] J.-H. Yoon, "Design and Fabrication of 1×8 DLP Array Antenna with Inset Feeding Structure in Private Network," *The Journal of The Korea Institute of Electronic Communication Sciences*, vol. 20, no. 3, pp. 473-480, June 2025.

[14] C.-Y. Gu, C. Yang, M.-S. Ju, D.-M. Jang, J.-S. Jang, J.-W. Jang, J.-K. Kim, T.-S. Kim, "Effects of Viscoelastic-Anisotropic Properties of Prepreg on Diagonal Warpage of Multilayer PCB Substrates," *IEEE Transactions on Materials for Electron Devices*, vol. 2, pp. 64-71, May 2025.

[15] R.R. Tummala, *Fundamentals of microsystems packaging*, 2nd ed., New York, McGraw-Hill, 2001.

[16] F. Hou, W. Wang, T. Lin, L. Cao, G.Q. Zhang, J.A. Ferreira, "Characterization of PCB Embedded Package Materials for SiC MOSFETs," *IEEE Transactions on Components, Packaging, and Manufacturing Technology*, vol. 9, no. 6, pp. 1054-1061, June 2019.

[17] D.J. Kearney, S. Kicin, E. Bianda, A. Krivda, "PCB Embedded Semiconductors for Low-Voltage Power Electronic Applications," *IEEE Transactions on Components, Packaging, and Manufacturing Technology*, vol. 7, no. 3, pp. 387-395, Mar. 2017.

[18] K. Li, B. Zhang, X. Li, F. Yan, L. Wang, "Electric Field Mitigation in High-Voltage High-Power IGBT Modules Using Nonlinear Conductivity Composites," *IEEE Transactions on Components, Packaging, and Manufacturing Technology*, vol. 11, no. 11, pp. 1844-1855, Nov. 2021.

[19] P. Adhikari, M. Ghassemi, "A Comprehensive Review of Mitigation Strategies to Address Insulation Challenges Within High-Voltage, High-Power-Density (U)WBG Power Module Packages," *IEEE Transactions on Dielectrics and Electrical Insulation*, vol. 31, no. 5, pp. 2676-2700, Oct. 2024.

[20] S.-W. Kim, "Identification of Partial Discharge Defect Detection in Cast-Resin Power Transformers Using Back-Propagation Algorithm," *Journal of Information and Communication Convergence Engineering*, vol. 22, no. 3, pp. 231-236, Sep. 2024.

[21] G.-Y. Lee, G.-S. Kil, "Insulation Defect Diagnosis Using a Ran-dom Forest Algorithm with Optimized Feature Selection in a Gas-Insulated Line Breaker," *Electronics*, vol. 14, no. 10, pp. 1940, May 2025.

[22] S. Seitz, T. Götz, C. Lindenberg, R. Tetzlaff, S. Schlegel, "Towards Generalizable Classification of Partial Discharges in Gas-Insulated HVDC Systems Using Neural Networks: Protrusions and Particles," *IEEE Transactions on Power Delivery*, vol. 39, no. 3, pp. 1491-1499, June 2024.

[23] Y. Cheng, H. La, C. Li, J. Huang, P.X. Liu, " A Decomposition-Based Improved Broad Learning System Model for Short-Term Load Forecasting," *Journal of Electrical Engineering & Technology,* vol. 17, pp. 2703–2716, June 2022.

[24] D. Soh, S.B. Krishnan, J. Abraham, L.K. Xian, T.K. Jet, J.F. Yongyi, "Partial Discharge Diagnostics: Data Cleaning and Feature Extraction," *Energies*, vol. 15, no. 2, pp. 508, Jan. 2022.

[25] G.V.R. Xavier, H.S. Silva, E.G. Da Costa, A.J.R. Serres, N.B. Carvalho, A.S.R. Oliveira, "Detection, Classification and Location of Sources of Partial Discharges Using the Radiometric Method: Trends, Challenges and Open Issues," *IEEE Access*, vol. 9, pp. 110787-110810, Aug. 2021.

[26] M. Bansal, A. Goyal, A. Choudhary, "A comparative analysis of K-Nearest Neighbor, Genetic, Support Vector Machine, Decision Tree, and Long Short Term Memory algorithms in machine learning," *Decision Analytics Journal*, vol. 3, pp. 100071, June 2022.

[27] C.W. Priananda, H.A. Illias, W.J. Keen, I.M.Y. Negara, "Hybrid Deep Learning Models for Enhanced Classification of Phase-Resolved Partial Discharge Patterns From High-Voltage Rotating Machine Insulation," *IEEE Transactions on Dielectrics and Electrical Insulations*, vol. 32, no. 5, pp. 3059-3067, Oct. 2025.

[28] A. Sharma, H. Devarajan, S. Govindarajan, T.B. Shanker, J.A.A. Rey, S. Nandi, "High-Confidence Classification of Partial Discharge Acoustic Signals Using Bayesian Networks for Uncertainty Quantification," *IEEE Transactions on Instrumentation and Measurement*, vol. 74, pp. 3506511, Jan. 2025.

[29] G.-Y. Lee, G.-S. Kil, S.-W. Kim, "Partial Discharge Defect Classification in Cast-Resin Transformers Using Machine Learning-Based Algorithms," *Journal of Electrical Engineering*, vol. 76, no. 6, pp. 565-573, Dec. 2025.

[30] S. Chouaibi, M.B. Ayed, Y.H. Kacem, S.A. Alshaya, F. Tounsi, "Fused CNN–LSTM for Within-Cycle Partial Discharge Classification From PRPD Images and Current Waveforms," *IEEE Access*, vol. 13, pp. 206504, Nov. 2025.

Gyeong-Yeol Lee received the B.Eng., M.Eng., and Ph.D. degrees in electrical engineering and high voltage engineering from National Korea Maritime and Ocean University, Korea in 2015, 2020, and 2025, respectively. He works in Korea Hydro & Nuclear Power Co., Ltd. Since 2016, his research interests have been in partial discharge diagnosis and analysis of gas-insulated switchgears and high-voltage transformers and precision high voltage and large current measurements.

Sung-Wook Kim received the B.Eng., M.Eng., and Ph.D. degrees in electrical engineering and high voltage engineering from National Korea Maritime and Ocean University, Korea in 2008, 2010 and 2017, respectively. He worked for R&D Center of Hyosung Corporation and was one of the members in charge of DGA project for 9 years. He is currently a professor at Silla University, Korea. His research interests are partial discharge and DGA measurements of high-voltage transformers and gas-insulated switchgears.

Received 22 January 2026